Lagrangian approach to the dynamics of dark matter-wave solitons

G. Theocharis,[1,5] P. Schmelcher,[1,2] M. K. Oberthaler,[3] P. G. Kevrekidis,[4] and D. J. Frantzeskakis[5]

[1]*Theoretische Chemie, Physikalisch-Chemisches Institut, INF 229, Universität Heidelberg, 69120 Heidelberg, Germany*
[2]*Physikalisches Institut, Philosophenweg 12, Universität Heidelberg, 69120 Heidelberg, Germany*
[3]*Kirchhoff Institut für Physik, INF 227, Universität Heidelberg, 69120 Heidelberg, Germany*
[4]*Department of Mathematics and Statistics, University of Massachusetts, Amherst, Massachusetts 01003-4515, USA*
[5]*Department of Physics, University of Athens, Panepistimiopolis, Zografos, Athens 157 84, Greece*

We analyze the dynamics of dark matter-wave solitons on a Thomas-Fermi cloud described by the Gross-Pitaevskii equation with radial symmetry. One-dimensional, ring, and spherical dark solitons are considered, and the evolution of their amplitudes, velocities, and centers is investigated by means of a Lagrangian approach. In the case of large-amplitude oscillations, higher-order corrections to the corresponding equations of motion for the soliton characteristics are shown to be important in order to accurately describe its dynamics. The numerical results are found to be in very good agreement with the analytical predictions.

PACS number(s): 03.75.Kk, 03.75.Lm, 05.45.Yv

I. INTRODUCTION

Dark solitons (DS's) are nonlinear excitations of the nonlinear Schrödinger (NLS) equation with repulsive interactions, which have been studied in the context of Bose-Einstein condensates (BEC's) both experimentally [1] and theoretically. In particular, as BEC's are confined in external trapping potentials, many studies dealt with the dynamics of dark solitons in harmonic [2–7] or optical lattice [8] potentials. Especially, in the former setup, it has been found that in elongated harmonic traps a dark soliton oscillates with frequency $\Omega/\sqrt{2}$ (Ω being the axial trapping frequency). This result is valid for both limiting cases pertaining to the two types of DS's—namely, the nearly black (deep) solitons [4]—and the grey (shallow) ones [3]; notice that it has recently been shown that, in the framework of the adiabatic approximation, the above result refers to DS's of arbitrary amplitudes [6]. Thermal [9] and dynamical [10] instabilities, mainly referring to rectilinear DS's, have been investigated as well. On the other hand, generalizations of the traditional rectilinear dark solitons, such as the ring dark solitons, have recently been proposed [11] (see, e.g., Refs. [12]). Systematic studies of the sound emission of dark solitons interacting with BEC inhomogeneities, as well as soliton sound interactions, have been performed [13]. It has been shown that quantum depletion of purely black (stationary) solitons [14] reduces their lifetime, as atoms tunnel in to fill up the notch at the soliton center. Finally, a method for the stabilization of dark solitons against dissipative losses, based on a parametric driving mechanism, has recently been proposed [15], which may pave the way for observing long-lived dark solitons in BEC's in future BEC experiments.

In this paper, we employ the Lagrangian approach devised in [16] to study the dynamics of dark solitons in trapped BEC's in the framework of the Gross-Pitaevskii equation (GPE). Our analytical consideration concerns all cases pertaining to quasi-one-dimensional (quasi-1D) dark solitons—namely, *rectilinear* ones as well as *ring* and *spherical* DS's—which are found as perturbative solutions with radial

symmetry of the GPE. The evolution equations for the soliton parameters (amplitude, velocity of the center, or radius) are derived analytically, and the respective results are compared with numerical ones, obtained by direct numerical integration of the respective GPE's (for the 1D and 2D settings). For harmonic traps, and solely in the 1D case, it is shown that the soliton oscillation on top of the Thomas-Fermi (TF) cloud is harmonic (with frequency $\Omega/\sqrt{2}$). This result is valid both for sufficiently deep dark solitons moving in regions around the trap center (with a length $\approx 25\%$ of the TF radius) and for shallower ones, oscillating in regions as wide as $\approx 85\%$ of the TF radius, in accordance with the results presented in [6]. We show that in the particular case of gray solitons, it is necessary to incorporate higher-order corrections to the evolution equations for the soliton parameters, in order to describe accurately the DS dynamics. In the higher-dimensional (cylindrical and spherical) settings, the effective (attractive) potential describing the soliton dynamics incorporates an additional (repulsive) curvature-induced logarithmic potential. Importantly, in the latter settings, these higher-order corrections are necessary for a satisfactory estimation of the critical radius for the formation of stationary ring DS's, as well as for a description of the nonlinear oscillation of the soliton radius up to the onset of the snaking instability. Finally, it is noted that our analysis does not rely on the specific form of the trap, as it can generally be applied in all cases where the soliton width (defined by the system's healing length) is sufficiently smaller than the spatial scale characterizing the external potential.

The paper is organized as follows: In Sec. II, the model and pertinent analytical considerations are presented, in Sec. III the analytical predictions are compared with direct numerical simulations, and, finally, in Sec. IV, the main results of this work are summarized.

II. ANALYTICAL RESULTS

A. Model and the effective perturbed NLS

Purely 1D dark solitons, in a 1D setting, as well as quasi-1D ones with radial symmetry—namely, cylindrical

(or ring) dark solitons—in a quasi-2D setting, and spherical dark solitons, in a 3D setting, can be described, in the framework of the mean-field theory, by the following normalized GPE (with repulsive interatomic interactions):

$$i\frac{\partial\psi}{\partial t} = -\frac{1}{2}\nabla^2\psi + |\psi|^2\psi + V(r)\psi, \tag{1}$$

where $\psi(r,t)$ is the mean-field wave fuction and the Laplacian is considered to be in the form

$$\nabla^2 = \frac{\partial^2}{\partial r^2} + \frac{(D-1)}{r}\frac{\partial}{\partial r}, \tag{2}$$

with $D=1,2,3$. In this setup, for $D=1$, Eq. (1) is actually a 1D GPE, describing a quasi-1D ("cigar-shaped") BEC, confined in a highly anisotropic trap with a very tight radial confinement; in this case, assuming that the longitudinal direction is x, the confining frequencies are $\omega_x \ll \omega_\perp$ and the variable r represents the longitudinal one—i.e., $r=x$. Similarly, for $D=2$, the GPE (1) describes a quasi-2D ("pancake") condensate, assumed to lie mainly in the x-y plane; in this case, the trap frequencies are such that $\omega_\perp \ll \omega_z$ and the variable r is the radial one—namely, $r=\sqrt{x^2+y^2}$. On the other hand, for $D=3$—i.e., in the purely 3D setting with spherical symmetry—the confining frequencies in the longitudinal and transverse directions are equal (taking the same value, say, ω) and the variable $r=\sqrt{x^2+y^2+z^2}$. In all cases ($D=1,2,3$), r is scaled in units of the fluid healing length $\xi=\hbar/\sqrt{n_0 g_{jD}m}$ (which also characterizes the size of the dark soliton), t in units of ξ/c (where $c=\sqrt{n_0 g_{jD}/m}$ is the Bogoliubov speed of sound), the atomic density is rescaled by the peak density n_0, and energy is measured in units of the chemical potential of the system $\mu=g_{jD}n_0$ (m is the atomic mass). Note that in the above definitions, g_{jD} (with $j=1,2,3$) correspond to the interaction strengths in 1D, 2D, and 3D; particularly, g_{1D} and g_{2D} are *effective* interaction strengths, which are obtained upon integrating the 3D interaction strength $g_{3D}=4\pi\hbar^2 a/m$ (a is the scattering length) in the transverse or the longitudinal directions, respectively. Finally, in the case of a harmonic trapping potential, the potential in Eq. (1) is $V(r)=(1/2)\Omega^2 r^2$, where the parameter Ω determines the magnetic trap strength and takes the values $\hbar\omega_x/g_{1D}n_0$, $\hbar\omega_\perp/g_{2D}n_0$, and $\hbar\omega/g_{3D}n_0$ for $D=1$, 2, and 3, respectively. Note that in the following analysis it is assumed that the width of the soliton ($\sim\xi$) is significantly smaller than the spatial scale characterizing the trap ($\Omega^{-1/2}$)—i.e., $\Omega\xi\ll1$. Generally speaking, our analysis does not rely on the specific form of the trapping potential. Thus, hereafter, we will proceed with the presentation of the analytical results assuming a general form of the trapping potential $V(r)$ and we will deal with the experimentally relevant case of the harmonic trap in the numerical simulations.

In order to treat analytically the dynamics of the traditional rectilinear dark solitons, we look for solutions of Eq. (1) of the form

$$\psi = \phi(r)\exp(-i\mu t)v(r,t), \tag{3}$$

where $\phi(r)\exp(-i\mu t)$ describes the background wave function, $v(r,t)$ describes the dark soliton, and μ is the normal-

ized chemical potential, which is connected to the number of atoms of the condensate. Below, without loss of generality, we will assume that $\mu=1$; note that for Ω of order $\sim10^{-2}$, and for typical values of trapping frequencies used in experiments, this choice leads, for a ^{87}Rb condensate, to a number of atoms, $N\sim10^3$. The stationary function $\phi(r)$ can be approximated in the TF framework [7] as

$$\phi(r) = \sqrt{1-V(r)} \tag{4}$$

in the region where $V(r)<1$ and $\phi(r)=0$ outside. On the other hand, substituting the ansatz (3) in Eq. (1), it is readily found that the soliton wave function $v(r,t)$ is governed by the evolution equation

$$i\frac{\partial v}{\partial t} + \frac{1}{2}\frac{\partial^2 v}{\partial r^2} - \phi^2(|v|^2-1)v = -\frac{\partial}{\partial r}\ln\phi - \frac{(D-1)}{r}\frac{\partial v}{\partial r}. \tag{5}$$

In the case of slowly varying external potentials under consideration, the logarithmic derivative of ϕ is apparently small [e.g., for the parabolic potential $V(r)=(1/2)\Omega^2 r^2$, it is of order of Ω, which is assumed to be a small parameter]. Additionally, in the special cases $D=2,3$, we may also assume that the cylindrical ($D=2$) and spherical ($D=3$) dark solitons are characterized by a large radius, such that $1/r=O(\Omega)$. Thus, it is clear that the right-hand side (RHS) and also part of the nonlinear terms of Eq. (5) can be treated as a perturbation. To obtain this perturbation in an explicit form, we first use Eq. (4) to approximate the logarithmic derivative of ϕ as

$$-\frac{\partial}{\partial r}\ln\phi \approx \frac{1}{2}\frac{dV}{dr}(1+V+V^2). \tag{6}$$

As we will show below, if the soliton is sufficiently deep and moves in a small region around the trap's minimum, its dynamics can be described analytically, with a good accuracy, taking into regard solely the leading-order term on the RHS of Eq. (6); in such a case and for a parabolic trap, the soliton dynamics is described by means of the equation of motion for a linear oscillator. Nevertheless, as we are interested in the case of shallow solitons as well, it is necessary to incorporate the higher-order corrections—i.e., the last two terms in the RHS of Eq. (6)—which play an important role in the description of the soliton motion.

Substituting now Eqs. (4) and (6) into Eq. (5), the following perturbed NLS equation is obtained:

$$i\frac{\partial v}{\partial t} + \frac{1}{2}\frac{\partial^2 v}{\partial r^2} - (|v|^2-1)v = P(v), \tag{7}$$

where the total perturbation $P(v)$ has the form

$$P(v) = \frac{1}{2}\left[2V(1-|v|^2)v + \frac{dV}{dr}\frac{\partial v}{\partial r} - \frac{(D-1)}{r}\frac{\partial v}{\partial r}\right]$$
$$+ \frac{1}{2}V(1+V)\frac{dV}{dr}\frac{\partial v}{\partial r}, \tag{8}$$

with the last two terms corresponding to the higher-order corrections in Eq. (6). In the absence of the perturbation $P(v)$, Eq. (7) represents a conventional defocusing NLS

equation, which possesses an exact analytical dark soliton solution of the form [17]

$$v(x,t) = B \tanh \zeta + iA, \qquad (9)$$

where $\zeta \equiv B(r - At)$ and the parameters A and B represent, respectively, the velocity and amplitude of the dark soliton, connected through the simple equation $A^2 + B^2 = 1$ (note that the limiting cases $B = 1$ and $B \ll 1$ correspond, respectively, to the stationary "black" soliton and the "gray" soliton, moving with a velocity near the speed of sound). It is clear that for $D = 1, 2, 3$ the solution (9) represents, respectively, a plane, a cylindrical (ring), or a spherical dark soliton; note that the cylindrical (spherical) soliton resembles an annular trough (dark spherical shell) on top of the TF cloud.

B. Lagrangian approach

To treat analytically the effect of the perturbation (8) on the dark soliton, we employ the adiabatic approximation of the Lagrangian perturbation theory for dark solitons [16]. According to this approach, the parameters of the dark soliton become slowly varying functions of time, but the functional form of the soliton remains unchanged. Thus, the soliton velocity, amplitude, and coordinate become $A \to A(t)$, $B \to B(t)$ and $\zeta \to \zeta = B(t)[r - r_0(t)]$, where $r_0(t)$ is the soliton center. Note that in the unperturbed case, $dr_0/dt \equiv A$, but in the general perturbed case under consideration, this simple relationship may not be valid (see below).

As has been shown in Ref. [16], the corresponding equations of motion of the soliton parameters $\alpha_j(t)$ [which is a generic name for $r_0(t)$ and $A(t)$] may be obtained as the Euler-Lagrange equations

$$\frac{\partial L}{\partial \alpha_j} - \frac{d}{dt}\left(\frac{\partial L}{\partial \alpha_j'}\right) = 2 \,\mathrm{Re}\left\{\int_{-\infty}^{+\infty} P^*(v) \frac{\partial v}{\partial \alpha_j} dr\right\}, \qquad (10)$$

where $\alpha_j' \equiv d\alpha_j/dt$ and $L = \int_{-\infty}^{+\infty} dr \mathcal{L}\{v\}$ represents the averaged Lagrangian of the dark soliton of the unperturbed NLS equation [namely, for $P(v) = 0$], with the Lagrangian density $\mathcal{L}$ being given by

$$\mathcal{L}\{v\} = \frac{i}{2}\left(v^* \frac{\partial v}{\partial t} - v \frac{\partial v^*}{\partial t}\right)\left(1 - \frac{1}{|v|^2}\right) - \frac{1}{2}\left|\frac{\partial v}{\partial r}\right|^2 - \frac{1}{2}(|v|^2 - 1)^2. \qquad (11)$$

Next we first substitute the ansatz (9) into Eq. (11) to find the averaged Lagrangian

$$L = 2\frac{dr_0}{dt}\left[-AB + \tan^{-1}\left(\frac{B}{A}\right)\right] - \frac{4}{3}B^3. \qquad (12)$$

Then, substituting Eq. (8) into Eq. (10) and taking into account that for any spatially slowly varying trapping potential $V(r)$ its higher-order derivatives may be omitted, we obtain the following evolution equations for the soliton parameters:

$$\frac{dr_0}{dt} = A\left[1 - \frac{1}{2}V(r_0)\right] - \frac{A}{4B^2}\left(\frac{5}{3} - \frac{\pi^2}{9}\right)\left(\frac{\partial V}{\partial r_0}\right)^2[1 - 2V(r_0)] \qquad (13)$$

and

$$\frac{dA}{dt} = -B^2\left[\frac{1}{2}\frac{\partial V}{\partial r_0} - \frac{(D-1)}{3r_0}\right] - \frac{1}{3}B^2 V(r_0)\frac{\partial V}{\partial r_0}$$
$$- B^2 \frac{\partial V}{\partial r_0}\left[\frac{1}{3}V^2(r_0) + \frac{1}{4}\left(\frac{2}{3} - \frac{\pi^2}{9}\right)\left(\frac{\partial V}{\partial r_0}\right)^2\right]. \qquad (14)$$

Equations (13) and (14) describe the DS dynamics, in both cases of nearly black solitons ($A \approx 0$ or $B \approx 1$) and gray ones (with arbitrary A or B). In the latter case, as we will show below, incorporation of the higher-order corrections in Eq. (6) is necessary to describe accurately the DS dynamics. In this respect, it is worth tracing the contribution of each term in the approximation, Eq. (6): First, the leading-order term gives rise to the first two terms on the RHS of Eqs. (13) and (14), while inclusion of the first-order term in Eq. (6) leads to the additional terms $\sim (\partial V/\partial r_0)^2$ in Eq. (13) and $\sim (\partial V/\partial r_0)V(r_0)$ in Eq. (14). Finally, incorporation of all terms in Eq. (6) leads to the final result of Eqs. (13) and (14).

Let us discuss now the most simplified version of Eqs. (13) and (14), corresponding to the above-mentioned leading order of approximation. In this case, the following equation for the soliton center can readily be derived:

$$\frac{d^2 r_0}{dt^2} = \left[-B^2\left(\frac{1}{2}\frac{\partial V}{\partial r_0} - \frac{(D-1)}{3r_0}\right) - \frac{A^2}{2}\frac{\partial V}{\partial r_0}\right]\left[1 - \frac{1}{2}V(r_0)\right]. \qquad (15)$$

This equation can further be simplified considering a nearly black soliton $B \approx 1$ ($A \approx 0$), moving in a vicinity of the trap's minimum (where $\mu \equiv 1 \gg V$). In such a case, Eq. (15) is reduced to the following Newtonian equation of motion for the soliton center:

$$\frac{d^2 r_0}{dt^2} = -\frac{\partial V_{\mathrm{eff}}}{\partial r_0}, \qquad (16)$$

where $V_{\mathrm{eff}}(r_0) = (1/4)\Omega^2 r_0^2 - \ln r_0^{(D-1)/3}$. Equation (16) recovers the well-known result [2,4–6] that in a 1D setting ($D = 1$), a nearly black soliton oscillates with frequency $\Omega/\sqrt{2}$ in the harmonic trap $V(x) = (1/2)\Omega^2 x^2$. Nevertheless, as the soliton becomes shallower—i.e., its amplitude B (velocity A) is decreased (increased)—it is clear that the time-dependent prefactors on the RHS of Eq. (15) come into play; at the same time, the soliton moves in regions where the value of the trapping potential becomes comparable to the chemical potential and, as a result, the soliton dynamics is accordingly modified. In this case, to describe the oscillatory motion of the gray soliton it is necessary to employ the full set of equations (13) and (14). Importantly, as we will show in the next section, the oscillation frequency of the gray soliton is again found to be $\Omega/\sqrt{2}$. Finally, it is worth mentioning that in the higher-dimensional settings with $D = 2, 3$ the equation of the soliton motion becomes nonlinear, even for nearly black solitons, due to the presence of the repulsive curvature-induced logarithmic potential; note that a similar equation of motion was first derived and discussed in [11], in the case of ring dark solitons ($D = 2$).
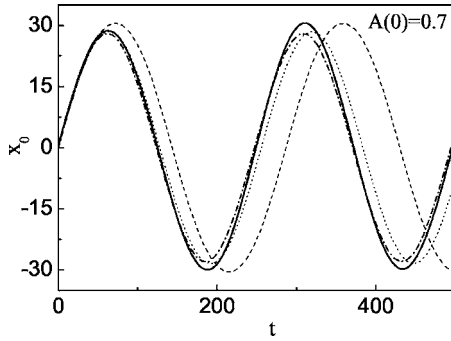
FIG. 1. Motion of the center of a dark soliton in a quasi-1D BEC confined in a parabolic trap with $\Omega = 0.035$ and TF radius ≈ 40. The soliton is initially placed at $x_0(0) = 0$, and its initial velocity is $A(0) = 0.7$. The almost coinciding solid and dash-dotted lines correspond, respectively, to the results of the direct numerical integration of the GPE and the analytical predictions of Eqs. (13) and (14). The dashed and dotted lines are results obtained from simplified versions of Eqs. (13) and (14), corresponding to the leading- [Eq. (15) for $D = 1$] and first-order approximations in Eq. (6) (see text).

III. NUMERICAL RESULTS

We have found that our analytical findings are in very good agreement with direct numerical simulations. In particular, we have systematically compared dark soliton trajectories, as predicted by Eqs. (13) and (14), with the ones obtained by direct numerical integration of the GPE (1) and present the relevant results in what follows.

As far as the simplest 1D case ($D = 1$) is concerned, we have considered a BEC confined in the harmonic trap $V(x) = (1/2)\Omega^2 x^2$ (with $\Omega = 0.035$) and we have performed a series of simulations, pertaining to solitons of the same initial position [$x_0(0) = 0$—i.e., at the trap center], but of different initial velocities $A(0)$, in the interval $(0, 0.8)$; note that larger values of A are physically less interesting, since for $A \approx 1$ the very shallow dark soliton is hardly distinguishable from sound. We have found that Eq. (16) describes accurately the soliton dynamics only for initial velocities $0 < A(0) < 0.2$, corresponding to soliton oscillations performed in $\approx 25\%$ of the TF radius. In the interval $0.2 < A(0) < 0.4$ (oscillations up to $\approx 40\%$ of the TF radius), it is necessary to take into account the first-order correction in Eq. (6) and employ the simplified version of Eqs. (13) and (14) [incorporating the terms $\sim (\partial V / \partial r_0)^2$ in Eq. (13) and $\sim (\partial V / \partial r_0) V(r_0)$ in Eq. (14)] to describe the soliton dynamics with sufficient accuracy: In particular the error in the estimation of the soliton oscillation frequency is reduced from $\approx 5\%$ to $\approx 1\%$ in the above-mentioned successive orders of approximation. Finally, for initial velocities $0.4 < A(0) < 0.8$ (amplitude of soliton oscillation up to $\approx 85\%$ of the TF radius), the dynamics of the dark soliton can only be described correctly using Eqs. (13) and (14). In the latter case, the error in the estimation of the soliton frequency is, respectively, reduced from $\approx 15\%$ to $\approx 3\%$ and, finally, to $\approx 1\%$. As an example, in Fig. 1, the soliton trajectory [for $A(0) = 0.7$] obtained by numerical integration of the GPE (1) is compared with the trajectories obtained by Eqs. (13) and (14) including simplified ver-

sions corresponding to above-mentioned different orders of approximation. Importantly, the numerically found oscillation frequency of the gray soliton was obtained to be $\omega_{osc} \approx 0.025$, which is in excellent agreement with the value $\Omega / \sqrt{2} = 0.024\,75$, which also corresponds to the prediction based on Eqs. (13) and (14) (compare the solid and dash-dotted curves in Fig. 1). This result is in accordance with the one obtained in [6], where it was predicted that the oscillation frequency of gray solitons is $\Omega / \sqrt{2}$. It is conjectured that the small discrepancy observed is merely due to nonadiabatic effects: In particular (as already suggested in [6]), deviation of the above-mentioned value of the oscillation frequency is due to the inhomogeneity-induced radiation (sound emission) of the dark soliton [13], which is not included in the present analysis [the original ansatz (9) used in the Lagrangian perturbation theory does not incorporate radiative effects]. Note that for deeper dark solitons [e.g., for $0 < A(0) < 0.2$], all three analytically predicted curves in Fig. 1—namely the dashed, dotted, and dash-dotted ones—almost coincide, in accordance with the results reported in earlier relevant works [2,4,5]. Finally, it is worth mentioning that additional simulations with different values of the trap strength Ω [but of the same order $O(10^{-2})$, so that the perturbative approach is valid] led to qualitatively similar results.

Let us now consider the 2D case—namely, the dynamics of cylindrical (ring) dark solitons. For the latter, the combination of the (attractive) harmonic trapping potential and the effective curvature-induced (repulsive) logarithmic potential [see Eq. (16)] indicates the existence of a critical radius R_{cr} for which a stationary ring exists, in contrast with their counterparts known in nonlinear optics [17]. Numerical simulations have confirmed the above prediction, and the critical radius has been found to be $R_{cr} = (\sqrt{1/2})\Omega^{-1}$, a result which is now compared with analytical predictions: While Eq. (16) predicts the value $(\sqrt{2/3})\Omega^{-1}$ (see also [11]), which leads to an error of $\sim 13.5\%$, the full set of equations (13) and (14) predicts the value $\sqrt{0.516\,18}\Omega^{-1}$, which is very close to the numerical one, with an error of 4%.

We have performed numerical simulations to compare the ring soliton trajectories found by the GPE (1) to the ones predicted by Eqs. (13) and (14) (as well as their simplified versions). As the ring radius oscillates between a minimum and a maximum value (see also [11]), we have considered solitons of sufficiently large minimum radius, so as to ensure the validity of the analytical approach (recall that we have assumed that $r^{-1} \sim \Omega \ll 1$). Additionally, in all cases the simulations were performed up to the onset of the snaking instability [10,17], which leads to the disintegration of ring solitons and the formation of vortices and vortex patterns [11] (see also [18] for recent reviews). In all cases, we found the analytical results to be in fairly good agreement with the numerical simulations, with an increasing accuracy from the simplified verions to the full model of Eqs. (13) and (14). As an example, in Fig. 2 we show the evolution of the radius $R \equiv r_0$ of a ring dark soliton in a condensate confined in the trap $V(r) = (1/2)\Omega^2 r^2$ (with $\Omega = 0.035$). The initial radius coincides with the minimum one—namely, $R_0 = R_{\min} = 18.2$—while the maximum radius is $R_{\max} = 22.2$. Only
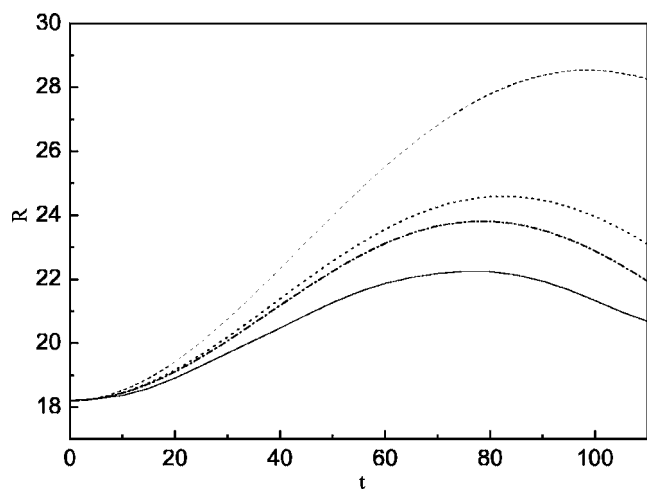
FIG. 2. Same as in Fig. 1, but for a cylindrical (ring) dark soliton with initial velocity $A(0)=0$. The initial value of the ring radius R is $R(0)=18.2 \equiv R_{min}$, while $R_{max}=22.2$. Note that at $t=110$, the snaking instability sets in.

$\approx 3/4$ of the oscillation period is shown (then, the snaking instability sets in). The evolution of the radius obtained by the numerical integration of the GPE (solid line) is directly compared to the ones obtained by Eqs. (13) and (14) (dash-dotted line), as well as to the simplified versions corresponding to the leading-order [dashed line, Eq. (16)] and second-order (dotted line) of approximation. It is worth mentioning that the error in the estimation of R_{max} is significantly reduced from 22% to 10.8% and, finally, to 7.2% in the successive orders of approximation.

IV. CONCLUSIONS

In conclusion, we have studied the dynamics of purely 1D and quasi-1D (cylindrical and spherical) dark matter-wave solitons in the framework of the Gross-Pitaevskii equation. Considering dark soliton solutions of the latter with radial symmetry, we have derived an effective perturbed NLS equation, which was then analyzed by means of the Lagrang-ian approach for dark solitons. Equations of motion for the soliton centers (radii in the 2D and 3D settings) have been obtained. For nearly stationary (black) dark solitons, moving close to the trap center (i.e., in regions where the chemical potential is significantly larger than the trapping potential) the soliton dynamics is successfully described by a Newtonian equation of motion. In this picture, the dark soliton behaves as a classical particle in the presence of a parabolic potential combined with a curvature-induced logarithmic potential (in 2D and 3D). Nevertheless, in the more general case of mobile (gray) dark solitons, oscillating in large regions on the Thomas-Fermi cloud, higher-order corrections in the evolution equations for the soliton characteristics have been found, which have to be incorporated to describe accurately the soliton dynamics. Numerical simulations for the 1D and 2D cases have been found to be in very good agreement with the analytical findings.

One of the main conclusions of this work is that the soliton oscillation frequency does not depend on the soliton amplitude, in accordance with the results reported recently in [6]. On the other hand, it should be noticed that in the presented approach, inhomogeneity-induced radiation effects (sound emitted by the dark soliton) are not encapsulated in the presented Lagrange averaging method. An analytical consideration of the radiation effects, as well as a detailed investigation of the soliton dynamics under their presence, is an interesting subject for future work. Finally, a more detailed study of the purely 3D case is another interesting subject for a future investigation.

[1] S. Burger, K. Bongs, S. Dettmer, W. Ertmer, K. Sengstock, A. Sanpera, G. V. Shlyapnikov, and M. Lewenstein, Phys. Rev. Lett. **83**, 5198 (1999); J. Denschlag, J. E. Simsarian, D. L. Feder, C. W. Clark, L. A. Collins, J. Cubizolles, L. Deng, E. W. Hagley, K. Helmerson, W. P. Reinhardt, S. L. Rolston, B. I. Schneider, and W. D. Phillips, Science **287**, 97 (2000); B. P. Anderson, P. C. Haljan, C. A. Regal, D. L. Feder, L. A. Collins, C. W. Clark, and E. A. Cornell, Phys. Rev. Lett. **86**, 2926 (2001); Z. Dutton, M. Budde, Ch. Slowe, and L. V. Hau, Science **293**, 663 (2001).

[2] Th. Busch and J. R. Anglin, Phys. Rev. Lett. **84**, 2298 (2000).

[3] G. Huang, J. Szeftel, and S. Zhu, Phys. Rev. A **65**, 053605 (2002).

[4] D. J. Frantzeskakis, G. Theocharis, F. K. Diakonos, P. Schmelcher, and Yu. S. Kivshar, Phys. Rev. A **66**, 053608 (2002).

[5] V. A. Brazhnyi and V. V. Konotop, Phys. Rev. A **68**, 043613 (2003).

[6] V. V. Konotop and L. Pitaevskii, Phys. Rev. Lett. **93**, 240403 (2004).

[7] F. Dalfovo, S. Giorgini, L. P. Pitaevskii, and S. Stringari, Rev. Mod. Phys. **71**, 463 (1999).

[8] P. G. Kevrekidis, R. Carretero-González, G. Theocharis, D. J. Frantzeskakis, and B. A. Malomed, Phys. Rev. A **68**, 035602 (2003); N. G. Parker, N. P. Proukakis, C. F. Barenghi, and C. S. Adams, J. Phys. B **37**, S175 (2004); P. J. Y. Louis, E. A. Ostrovskaya, and Yu. S. Kivshar, J. Opt. B: Quantum Semiclassical Opt. **6**, S309 (2004); G. Theocharis, D. J. Frantz-

eskakis, R. Carretero-González, P. G. Kevrekidis, and B. A. Malomed, Phys. Rev. E **71**, 017602 (2005).

[9] P. O. Fedichev, A. E. Muryshev, and G. V. Shlyapnikov, Phys. Rev. A **60**, 3220 (1999); A. E. Muryshev, G. V. Shlyapnikov, W. Ertmer, K. Sengstock, and M. Lewenstein, Phys. Rev. Lett. **89**, 110401 (2002).

[10] D. L. Feder, M. S. Pindzola, L. A. Collins, B. I. Schneider, and C. W. Clark, Phys. Rev. A **62**, 053606 (2000); J. Brand and W. P. Reinhardt, *ibid.* **65**, 043612 (2002); P. G. Kevrekidis, G. Theocharis, D. J. Frantzeskakis, and A. Trombettoni, *ibid.* **70**, 023602 (2004).

[11] G. Theocharis, D. J. Frantzeskakis, P. G. Kevrekidis, B. A. Malomed, and Yu. S. Kivshar, Phys. Rev. Lett. **90**, 120403 (2003).

[12] Ju-Kui Xue, J. Phys. A **37**, 11223 (2004); L. D. Carr and C. W. Clark, e-print cond-mat/0408460.

[13] N. G. Parker, N. P. Proukakis, M. Leadbeater, and C. S. Ad-

ams, Phys. Rev. Lett. **90**, 220401 (2003); J. Phys. B **36**, 2891 (2003); N. P. Proukakis, N. G. Parker, D. J. Frantzeskakis, and C. S. Adams, J. Opt. B: Quantum Semiclassical Opt. **6**, S380 (2004).

[14] J. Dziarmaga and K. Sacha, Phys. Rev. A **66**, 043620 (2002); J. Dziarmaga, Z. P. Karkuszewski, and K. Sacha, J. Phys. B **36**, 1217 (2003); C. K. Law, Phys. Rev. A **68**, 015602 (2003).

[15] N. P. Proukakis, N. G. Parker, C. F. Barenghi, and C. S. Adams, Phys. Rev. Lett. **93**, 130408 (2004).

[16] Yu. S. Kivshar and W. Królikowski, Opt. Commun. **114**, 353 (1995).

[17] Yu. S. Kivshar and B. Luther-Davies, Phys. Rep. **298**, 81 (1998).

[18] P. G. Kevrekidis and D. J. Frantzeskakis, Mod. Phys. Lett. B **18**, 173 (2004); P. G. Kevrekidis, R. Carretero-González, D. J. Frantzeskakis, and I. G. Kevrekidis, Mod. Phys. Lett. B **18**, 1481 (2004).